Design of a buck converter battery charging controller in PV plant

Lylia LARBI
Laboratoire de technologie industrielle et de l'information, Université de Béjaia
Bejaia, Algeria
lylia.larbi06@gmail.com

Slimane HADJI
Laboratoire de technologie industrielle et de l'information, Université de Béjaia
Bejaia, Algeria
mail.hadji@gmail.com

Abdelhakim BELKAID
Laboratoire de technologie industrielle et de l'information, Université de Béjaia
Bejaia, Algeria
belaid08@yahoo.fr

Ilhami COLAK
Department of Electrical & Electronics Engineering
Nisantasi University
Istanbul, Turkey
ilhcol@gmail.com

Ramazan BAYINDIR
Department of Electrical & Electronics Engineering
Gazi University
Ankara, *Turkey*
bayindir@gazi.edu.tr

***Abstract*— A smart grid can be made up of electrical system components and communication networks connected by complex relationships. The power system considered in this study is constructed by 135W panels with battery storage. This paper presents the design of a battery charging circuit by a maximum power point tracking algorithm MPP based on the perturb and observe method. This photovoltaic system associated with a DC-DC boost converter driven by the P&O technique in order to improve the efficiency and the output voltage under illumination change between 500-1000W/m^2. A Buck converter controlled with a PID regulator and supplied by the output voltage of the first converter form a battery charging circuit.**

The goal of this work is to function the PV system in variable environmental conditions to have a good efficiency and minimize the overall costs of the system as well as reduce the losses of the battery and improve its condition and increase its life cycle.
This system is studied and simulated in MATLAB/SIMULINK environment.

Keywords*— Smart grid; Photovoltaic; boost converter; buck converter; battery charger.

I. INTRODUCTION

Electricity is a critical aspect of a country's commercial development. The shift from a traditional to a mechanical society has produced an energy black hole, with approximately 1.3 billion people throughout the world without regular access to electricity for cooking and heating [1], more than 2.7 billion people still depend bioenergy sources such as wood, agricultural wastes, animal dung, and so on [2]. The marginal population in developing nations suffers the most from power shortages, which have a negative impact on their health and economic progress. Many of these areas have ample renewable energy sources, such as bio-mass, wind, and the sun. Owing to the global energy problem and environmental concerns, governments all over the globe have been focusing on green technology in recent years, with solar energy emerging as one of the most powerful forms of renewable energies [3]. The solar system is utilized in connexion with batteries, which operate as an energy soak pit and are employed when the PV system alone is unable to provide the needed electricity. Batteries are the most powerful and cost-effective source of house lighting in isolated and rural settings. It is, nevertheless, frequently employed in battery electric cars. The PV system has non-linear P/V and I/V curves and is highly reliant on atmospheric variables, such as solar irradiation and temperature [4]. Changes in irradiance and temperature affect voltage and current, causing the PV panel's maximum usable power to fluctuate. As a result, the system's conversion efficiency is only 7-19%, and manufacturing costs rise. The PV system will function at MPP in changing air conditions to avoid this limitation. Different MPPT algorithms [5], including as perturbation and observation (P&O) [6], incremental conductance (IC) [7], and fuzzy logic (FL) [8], have been explored and developed so far to run a PV panel. The MPPT control uses the output of the PV system in terms of current and voltage to produce a PWM trigger signal for the boost converter power switch. The most popular techniques for charging a battery are constant voltage and constant current [9]. A buck converter controlled using PID regulator is employed as the charge circuit to make the voltage and current invariant to the connected load. Because of its low cost, simple design, and high performance, the PID controller is extensively utilized in numerous industrial appliances like electric cars, process control, and power systems [10]. The suggested P&O-based PV system is for battery charger circuit and system response study under various meteorological conditions. The ability to remotely monitor and manage multiple system components is a key aspect of this novel MPPT approach. It lists the battery-recharging stations that are available in lonesome that are not yet linked to the network. A digital control strategy has been implemented for a buck dc-dc converter that charges a battery

using solar energy generated in various atmospheric conditions.

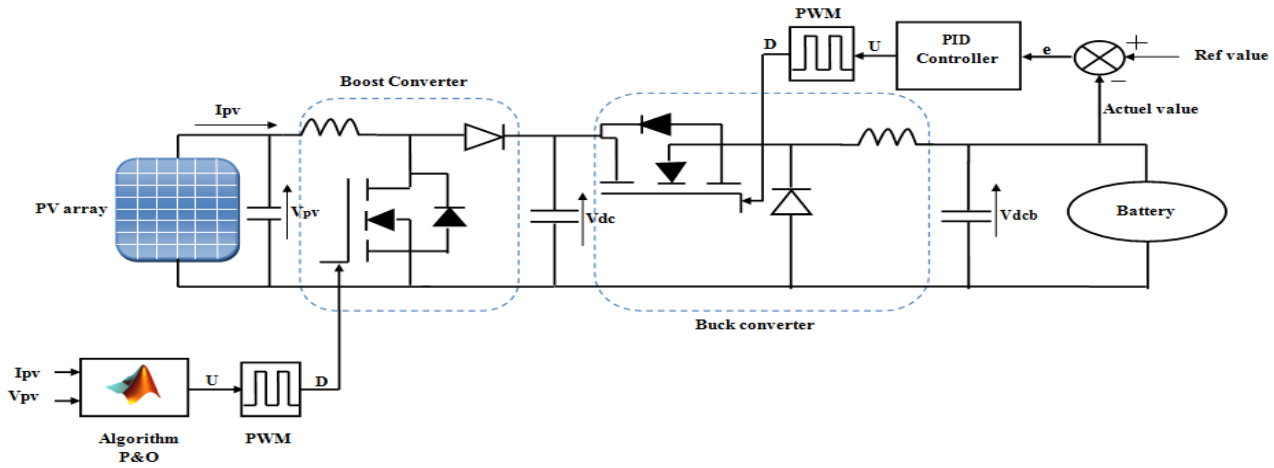

Fig.1. Battery charger for PV system.

The MPPT-based PV system is used to charge the battery and ultra-condensator separately, and it describes the improvement in charge rate compared to charging without MPPT.

The objectives of this work is to run the solar panel at its maximum output power in varying weather circumstances in order to boost efficiencies and reduced expenses, as well as to deliver appropriate current and voltage to quickly change the battery, decrease losses, and extend the battery life cycle. The MPPT algorithm (P&O) is used, and the most suited option for maximum photovoltaic power tracking is chosen. A PV generator, a dc-dc converter, a battery, and a PID controller are the primary components. MATLAB/Simulink is used to implement this novel realization.

II. DESCRIPTION OF PV SYSTEM

The PV system's performance and efficiency are entirely reliant on the different panel types as well as different climatic conditions, including non-uniform insolation and temperature variations. A PV system's P/V and I/V curves.The P/V and I/V parameters of an SPV system are determined at a constant ambient temperature of 25°C and variable solar irradiance. Figure 3 shows the P/V and I/V characteristics of a solar power system under fixed temperature of 25 °C and variable irradiance, respectively, while Figure 4 shows the P/V and I/V characteristics of a solar power system under variable temperature and constant solar insolation of 1000 W/m^2. It depicts the P-V and I-V properties of an SPV exposed to different temperatures while maintaining the solar irradiation constant at 1000 W/m2.When compared to the effect of a change in solar irradiance, the effect of a variable temperature, as illustrated in Figs. 3 and 4, has less influence on the properties of the SPV system. For the battery charge circuit based on an SPV system, the study is focused on a constant solar temperature of 25 °C and a varied insolation of 500 to 1000 W/m^2.

A. A solar cell's mathematical equation

The equivalent electric circuit of a solar cell may be modelled in a variety of ways, including using a diode model in the work presented. In Fig. 2, a simplified circuit is depicted, and the I-V relationship is:

$$I = Iph - I0\left\{e\frac{q(V+RsI)}{AKT} - 1\right\} - \frac{V+RsI}{Rsh} \qquad (1)$$

At which I_{ph} indicates the photocurrent, I_d indicates the current across the diode, I_{sh} signifies the parallel current, R_{sh} indicates the parallel resistance, R_s indicates the series resistance, I is the net PV current, V is the tension through the SPV, I_0 is the inverse diode current, q denotes the electron charge, A represents the curve adjustment factor, and K signify the Boltzmann constant (1.38×10^{-23} J/K).

B. Modeling of a PV module

When R_{sh} is supposed to be infinite and the slope of the I/V curve is zero at short circuit; the last term of (1) can be removed. I_{ph} is already replaced by the short-circuit current I_{SC}:

$$I = Isc - I0\left\{e^{\frac{q(V+RsI)}{AKT}} - 1\right\} \qquad (2)$$

The efficient utilization of solar energy in a PV module (2)

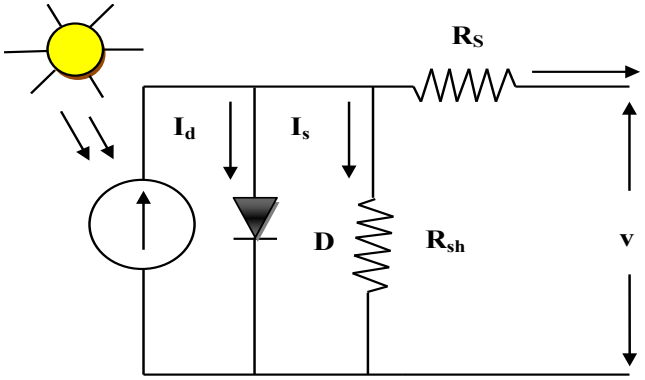

Fig.2. Single diode model PV cell

$\frac{q(V+RsI)}{AKT}$ Is altered and replaced with $\frac{q(V+RsI)}{NsAKT}$, In a crystalline type PV module, Ns specifies the overall number of solar cells placed back to back. Yields (3):

$$I = Isc - I0\left\{e^{\frac{q(V+RsI)}{NsAKT}-1}\right\} \quad (3)$$

When a PV module is in the open-circuit state, I=0 As well as the term $\frac{q}{NsAKT}$ (3) will be written in the following manner:

$$\frac{q}{AKT} = \frac{\ln(\frac{Isc}{I0}+1)}{Voc} \quad (4)$$

V_{OC} stands for open-circuit voltage of the module. The current may be calculated using (3) and (4) as follows:

$$I = Isc\left\{1 - \frac{I0}{Isc}(e^{\ln(\frac{Isc}{I0}+1)(\frac{V+RsI}{Voc}} - 1\right\} \quad (5)$$

Where k =Isc/I0 and obtained (6) after solving (5):

$$I = Isc\left\{1 - \frac{1}{K}(K+1)^{\frac{V+RsI}{Voc}} + \frac{1}{K}\right\} \quad (6)$$

k is usually fairly high as I_{SC} is significantly bigger than I_O. For a simplified I–V relationship, the following terms in (6) can be ignored:

$$I = Isc\left\{1 - k^{\frac{(V+RsI)}{Voc}-1}\right\} \quad (7)$$

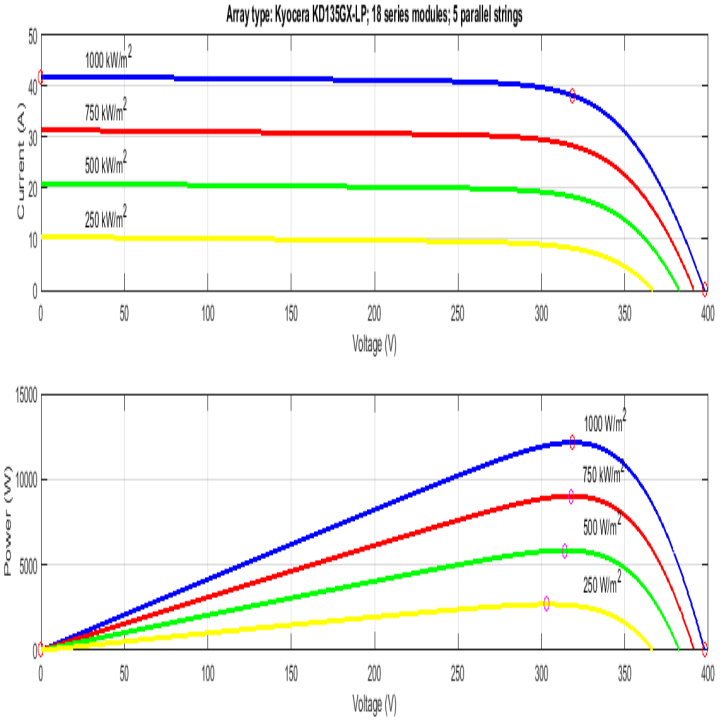

Fig 3: I/V and P/V curves of array at 25 deg.C

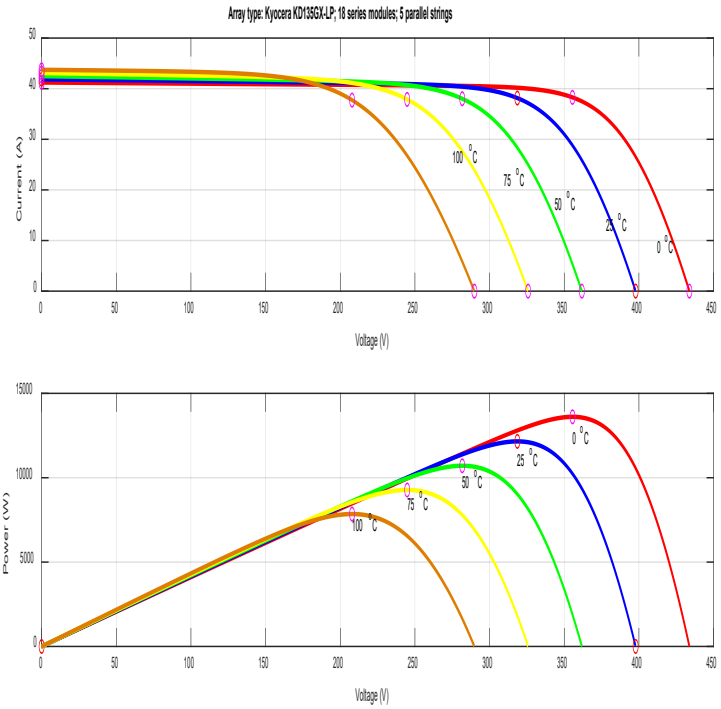

Fig 4: I/V and P/V curves of array at 1000 W/m^2

III. TECHNIQUES FOR PEAK POWER TRACKING

A commercial PV principal disadvantage is its lower conversion efficiency. Accordingly, the MPPT method is used to improve system efficiency. As shown in Fig. 5, an SPV system's greatest efficiency is predicted when it Works at MPP .

A. Perturbation & observation (P&O)

The suggested P&O algorithm is a powerful MPPT algorithm for a PV system operating at MPP. The advantages of this approach are that it is simple to execute and calculate, and it has a 99 % efficiency rate. The flowchart and structure of this approach are depicted in the diagrams below

P&O is based on a panel voltage perturbation. The P/V characteristic of a PV panel, as exposed in Fig. 6, shows that while working at left of the MPP, it increases/decreases with increasing/decreasing the voltage V, whereas on the right side of MPP, it decreases/increases. The step size of the perturbation can be lowered to reduce oscillations.

The following is a diagram of the whole P&O algorithm:

P&O algorithm:

Step 1: Begin

Step 2: Read variables V (n) and I (n).

Step 3: Compute power: P (n) = V (n)* I (n).

Step 4: Call from the memory P (n-1) and V (n-1).

Step 5: Compute the power variation ‘dP’ and the voltage variation ‘dV’ using: dV= V(n) - V (n-1) and dP= P(n) - P (n-1).

Step 6: If dP= 0, Then no variation in duty cycle is required and GO TO Step 7.

Else If (dP* dV) > 0, Then augment the duty cycle by ΔD and GO TO Step 7.

Else diminish the duty cycle by ΔD and GO TO Step 7

Step 7: return.

Fig 5: P/V and I/V curve for MPP

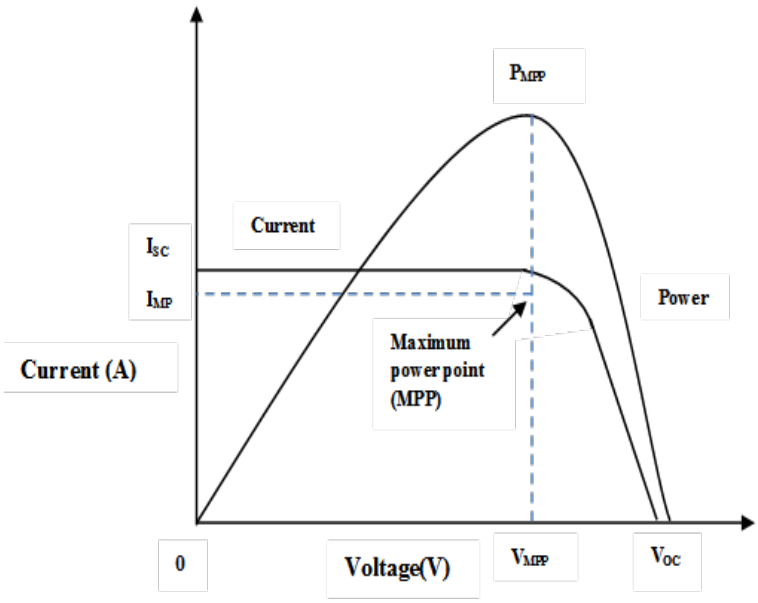

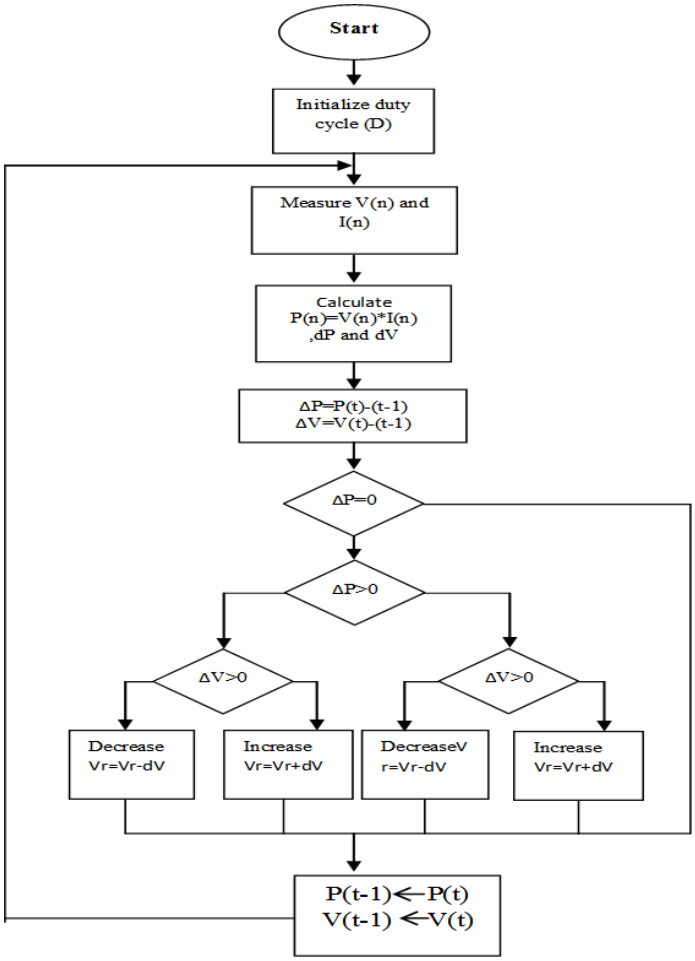

Fig 6: Structure for MPPT technique P&O

IV. DESIGN OF DC-DC CONVERTERS

The PV is designed to function at MPP for maximum power production. The power converter is controlled with the appropriate D to track the MPP of the SPV. In order to measure MPP, D must alter in accordance with changes in solar insolation. Various DC-DC converter configurations have been examined thus far, with the boost converter being the most often adopted and considered in the current study due to its lower complication and greater reliability, as illustrated in Fig. 1.

A. Boost DC-DC converter

For boost converter functioning, a MOSFET is used as a switching device. MOSFETs switch on and the diode becomes reverse biased over the time period t<0<DT. During this time interval, the voltage $V_L = V_{in}$ is applied to the inductor L. Due to forward bias, the MOSFET falls into an off state and the diode gets into an on state within the time period Dt< t<T. In this case, the output voltage $V_{out} = V_{dc} = V_{in} + V_L$. The total energy retained by L in a steady state condition must match the energy released by L during a switching phase. The following formulae are used to calculate the parameters L and C of the boost converter: [16]

$$V_{out} = V_{dc} = \frac{V_{in}}{(1-D)} \quad (8)$$

$$I_{out} = (1-D)I_{in} \quad (9)$$

$$L = \frac{V_{in} * D}{f_s * \Delta I} \quad (10)$$

$$C = \frac{I_{out} * D}{f_s * \Delta V} \quad (11)$$

Where C is the capacitor, I_{out} is the boost converter's current output, ΔI signifies the inductor current ripple, ΔV represents the output voltage ripple, f_s indicates the power device's switching frequency, and I_{in} is the boost converter's input current.

B. Buck converter

Buck converter provides output voltages that are lower in magnitude than the input source. The MOSFET turns on for 0<t<DT while the diode is off, charging the inductor with a voltage $V_L = V_{dc}-V_{dcb}$. For DT<t<T, the MOSFET switches off, and the diode enters conduction, with the voltage produced through the inductor changing to $V_L=-V_{dcb}$). To provide a constant current and voltage when charging a battery. As illustrated in Fig. 1, PI-PID controllers are designed to create a regulated reference signal u for the PWM generator, which provides the updated D to the buck converter. The parameters L and C of a dc-dc buck converter are computed using the following formulas [13-14]:

$$V_{dcb} = D * V_{dc} \quad (12)$$

$$L = \frac{V_{dcb} * (1 - D)}{f_s * \Delta I_b} \quad (13)$$

$$C = \frac{V_{dcb} * (1 - D)}{8 * L * f_s * \Delta V_{dcb}} \quad (14)$$

Where V_{dcb} is the buck converter's output voltage, V_{dc} is the buck converter's input dc supply voltage, ΔI_b is the ripple of the inductor current, and ΔV_{dcb} is the ripple of the output voltage.

C. Methodology of control

The design methods of classical ZN-PI and ZN-PID controllers for voltage regulation with buck converter are provided in this part. A generalized PID controller's differential equation is commonly expressed in 'parallel form' or 'ideal form,' as indicated by (15) or (16) accordingly.

$$u(t) = K_p e(t) + K_I \int e(t)dt + K_D \dot{e}(t) \quad (15)$$

$$u(t) = K_p \left[e(t) + \frac{1}{T_I} \int e(t)dt + T_D \dot{e}(t) \right] \quad (16)$$

Where K_P K_I and K_D are PID gains, T_I and T_D are integral and derivative time constants, and u and e are the controller's output and input, i.e. error signal, respectively. The PID parameters are quantified using the ZN tuning approach [15] which employs the following relations:

For PI control:
$K_P = 0.75K_u$, $TI = T_u / 1.2$, $K_I = K_P/T_I$

For PID control:
$K_P = 0.6K_u$, $K_I = K_P/T_I$ and $K_D = K_P/T_D$, $T_I = T_u/2$, $T_D = T_u/8$,
Where K_u and T_u are the system's ultimate gain and time respectively [11-12].

TABLE I.

ZN-PI, ZN-PID parameters

Controller	K_P	K_I	K_D	*Ku and Tu*
ZN-PI	0.955	104	–	Ku=1.27 & Tu=1.1×10^{-3}
ZN-PID	0.015	134	1.09×10^{-6}	Ku=1.27 & Tu=1.1×10^{-3}

V. Results and Discussion

MATLAB/Simulink software was used to define and simulate the full system shown schematically in Fig. 1. Table 1 lists the numerical values utilized in the simulation. A PV panel with a top power of 135 W, a boost, and a buck converters working as a charge controller for a battery and running at fs of 150 kHz make up the planned system.

TABLE II. Numerical values for simulation,

System	*Symbols*	*Values*
SPV	Voc/module Isc/module Cells in module Ns Np	30.80V 8.2329A 1 1 1
BOOST	fs L C	150kHz 2.3×10^{-3}H 440×10^{-6}F
BUCK	fs L C	150kHz 820×10^{-6}H 200×10^{-6}F

The MPPT techniques are used to operate the SPV system at MPP and an in-depth comparative transient analysis of the dynamic response in terms of the output power of the PV corresponding to MPP, as well as the voltage and current of the boost converter, has been performed below quickly changing solar irradiance. The power has reached its maximum value, and the variation of the increment step D affects the oscillations around the maximum power point, as shown in Figure 8. The acquired data demonstrates the control's effectiveness in tracking the maximum power point. When it comes to system stability, it's worth noting that if the duty cycle step is significant, the MPPT algorithm will respond quickly to changes in the system's operating circumstances, but stability losses will grow.

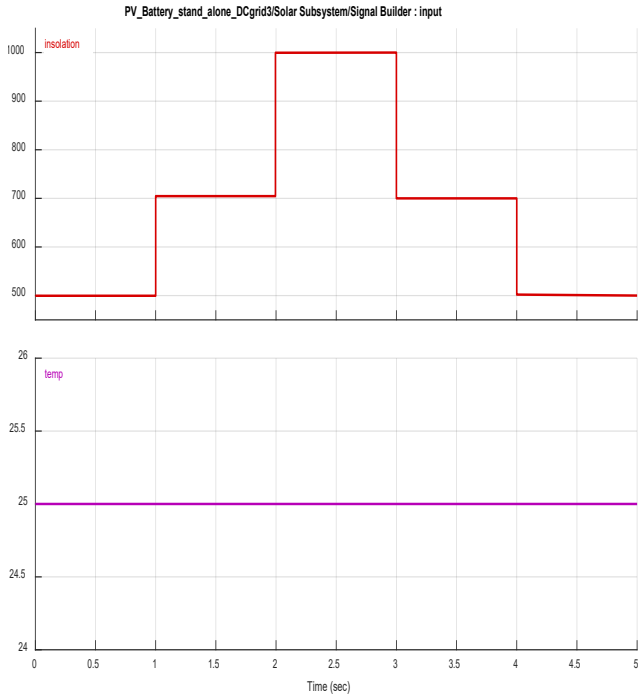

Fig 7: curve of a system input signal

According to the results obtained, the current and power curve follows the same trajectory as the input signal which allows to have a good power efficiency for this system.

The results of the simulations are shown below:

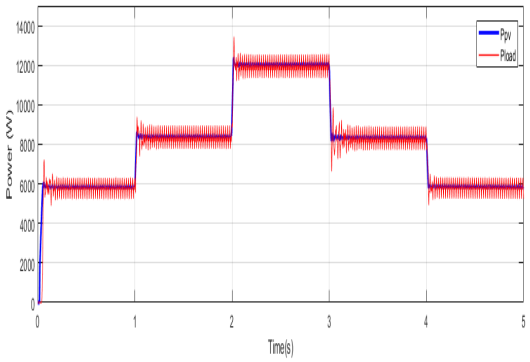

Fig 8: Curve of output power and input power of system using P&O

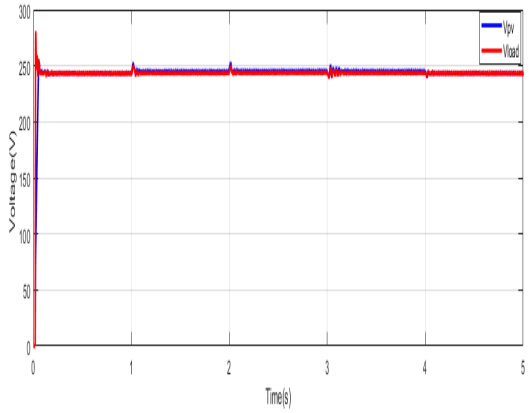

Fig 9: Curve of output voltage and input voltage using P&O

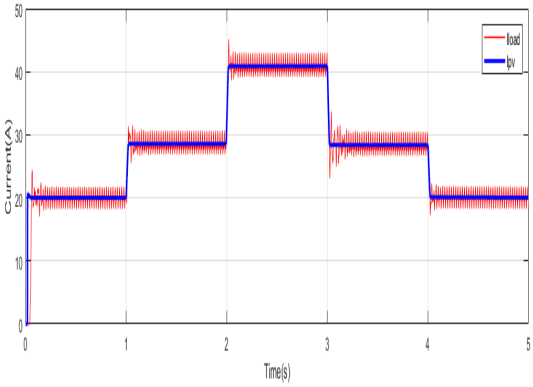

Fig 10: Curve of output current and input current of system using P&O

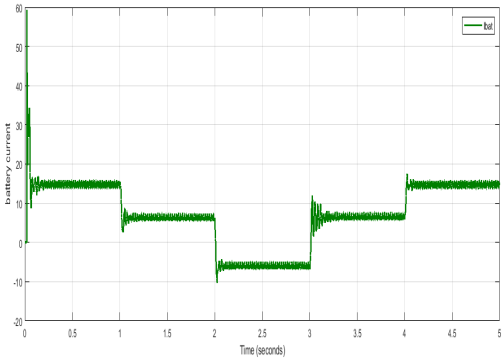

Fig 11: Curve of output current battery system using P&O

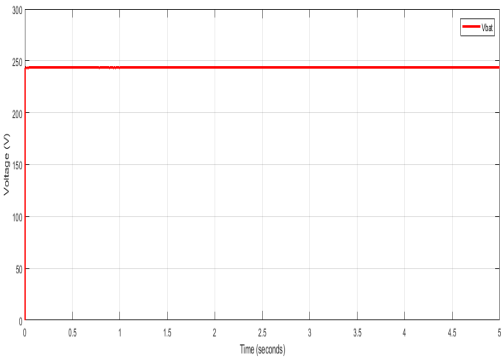

Fig 12: Curve of output voltage battery system using P&O

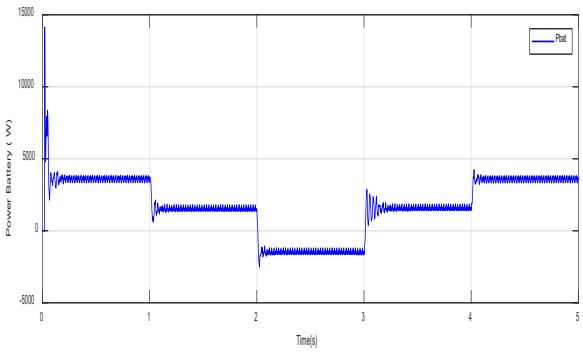

Fig 13: Curve of output power battery system using P&O

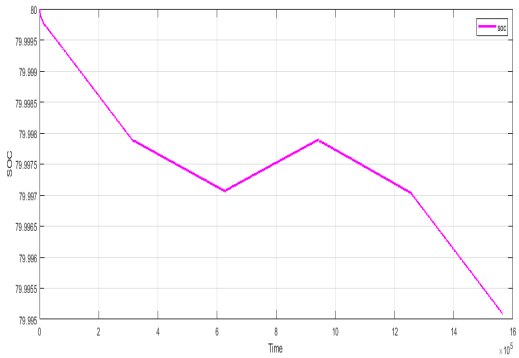

Fig 13: Curve of SOC battery system using P&O

VI. CONCLUSION

This study looked at the performance of a 135W PV system under various sunshine situations. To run the PV system at MPP, a special P&O strategy with fewer restrictions was designed for the battery charging circuit. The findings reveal that the P&O method has a greater maximum efficiency. The tracking speed is efficient under various air circumstances, and there is no fluctuation from MPP. As a result, in terms of boost converter voltage and current, which is the most significant aspect, the P&O technique surpasses the other strategies. In contrast to the current literature, which uses a PI controller to charge a battery, this study compares ZN-PI and ZN-PID driven buck converters as a battery charging circuit. As a consequence, the P&O-based SPV system, which employs PID control as a charge controller to charge a battery, may be said to be exceptionally successful for rapid and efficient charging, lowering losses and prolonging the battery's life cycle. The performance of a PID-controlled charge controller to charge a battery powered by a partially shaded PV system will be the focus of future research. If there is suitable assistance with the study material, the established system may be produced and implemented realistically.

REFERENCES

[1] G. Adinolfi, G. Graditi, P. Siano, A. Piccolo, 2015. Multi-Objective optimal design of photovoltaic synchronous boost converters assessing efficiency, reliability and cost savings. IEEE Trans. Ind. Info. 11 (5), 1038–1048.

[2] V. Agarwal, H. Patel, 2010. MATLAB-based modeling to study the effects of partial shading on PV array characteristics. IEEE Trans. Energy Convers. 23, 302–310.

[3] S. Hattori, H. Eto, F. Kurokaw, “High Power Density Battery Charger for Plug-In Micro EV”, International Journal of Renewable Energy Research (IJRER), Vol. 08, No. 2, pp. 1006-1015, 2018..

[4] A. Belkaid, I. Colak and K. Kayisli, "A comprehensive study of different photovoltaic peak power tracking methods," 2017 IEEE 6th International Conference on Renewable Energy Research and Applications (ICRERA), San Diego, CA, pp. 1073-1079, 2017.

[5] Chen, P.-C., Chen, P.-Y., Liu, Y.-H., Chen, J.-H., Luo, Y.-F., 2015. A comparative study on maximum power point tracking techniques for photovoltaic generation systems operating under fast changing environments. Sol. Energy. 119, 261–276

[6] S. A. M. Abdelwahab, A. M. Hamada, W. S. E. Abdellatif, “Comparative Analysis of the Modified Perturb & Observe with Different MPPT Techniques for PV Grid Connected Systems”, International Journal of Renewable Energy Research (IJRER), Vol. 10, No. 1, pp. 155-164, 2020.

[7] Elgendy, M.A., Zahawi, B., Atkinson, D.J., 2013. Assessment of the incremental conductance maximum power point tracking algorithm. IEEE Trans. Sustain. Energy. 4,108–117

[8] Algazar, M.M., AL-monier, H., EL-halim, H.A., Salem, M.E., EI, K., 2012. Maximum power point tracking using fuzzy logic control. Elec. Pow. Energy Syst. 39, 21–28

[9] P. K. Pathak, A. K. Yadav. Design of battery charging circuit through intelligent MPPT using SPV system. Sol. Energy. 178, 79–89, 2019.

[10] S. Nayak, S. K. Kar, S. S. Dash, “Improved Sunflower Optimization Algorithm Tuned Adaptive Type -2 Fuzzy PID Controller for Frequency Regulation of Renewable Power Integrated Hybrid Distributed Power System”, International Journal of Renewable Energy Research (IJRER), Vol. 11, No. 4, pp. 1928-1938, 2021.

[11] Neath, M.J., Swain, A.K., Madawalaand, U.K., Thrimawithana, D.J., 2014. An optimal PID controller for a bidirectional inductive power transfer system using multiobjective genetic algorithm. IEEE Trans. Pow. Elec. 29 (3), 1523–1531.

[12] Yadav, A.K., Gaur, P., 2016b. An optimized and improved STF-PID speed control of throttle controlled HEV. The Arabian Journal for Science and Engineering. 41 (9),3749–3760.

[13] Hart, D.W., 2011. Power electronics. McGraw Hill Edu.

[14] O. Kaplan and F. Bodur, "Super Twisting Algorithm Based Sliding Mode Controller for Buck Converter with Constant Power Load," 2021 9th International Conference on Smart Grid (icSmartGrid), 2021, pp. 137-142, doi: 10.1109/icSmartGrid52357.2021.9551244.